HYPORHEIC EXCHANGE ALONG A RIVER BELOW A DAM

ALESSANDRA MARZADRI, DANIELE TONINA

Center for Ecohydraulics Research, University of Idaho, 322 E. Front Street, suite 340
Boise, Idaho, 83702, USA

JAMES A. MCKEAN
Rocky Mountain Research Station, US Forest Service 322 E. Front Street, suite 401
Boise, Idaho, 83702, USA

MATT TIEDEMANN
Center for Ecohydraulics Research, University of Idaho, 322 E. Front Street, suite 340
Boise, Idaho, 83702, USA

Hyporheic exchange is an important mechanism for solute mixing between river waters and shallow groundwater in streambed sediment. The hyporheic zone also provides an important ecotone for benthic species, including macro-invertebrates, microorganisms, and parts of some fish life stages. Most hyporheic analyses are limited in scope and performed at the reach scale. This research investigates hyporheic flow induced by streambed topography at the valley-scale under different flow discharges. We use a pumping model to predict hyporheic exchange along a 37km long reach of the Deadwood River for different flow releases from Deadwood Reservoir and at different discharges from its tributaries. Hyporheic flow is primarily driven by near-bed pressure variations induced by flow and river geometry interaction in gravel bed rivers. We separate the contribution due to small-scale topography, which mainly affects dynamic head variations, and that of large-scale topography, which chiefly controls piezometric head variations. We model the former as head variations due to dune-like bedforms and the latter with the water surface elevation predicted in a 1-dimensional surface water hydraulic model. Superposition of these two energy-head components provides the boundary condition for modeling hyporheic flows, which are solved as Darcy's fluxes. In our study river, the hyporheic model shows that the mean hyporheic fluxes are mainly driven by small-scale streambed topography with limited effects of stream discharge.

1 INTRODUCTION

Hyporheic exchange is the primary mechanism which brings oxygen-rich and solute-laden surface water within the streambed sediment [1-4]. Similarly, it brings reduced-element laden waters from the low-oxygen concentration environment of the streambed sediment to the surface water environment. This mixing creates chemical and physical gradients that sustain a rich ecotone [5]. Spatial and temporal variations of near-bed energy heads, sediment hydraulic conductivity, alluvial area, turbulence, sediment transport and the density gradient between stream and pore waters drive stream water into the streambed sediment in downwelling areas [3, 6]. These fluxes can extend vertically and laterally, depending on stream sinuosity, alluvial sediment stratification and bedrock outcrop. They can be classified as fluvial hyporheic fluxes, which mainly extend laterally within the channel wetted areas, parafluvial fluxes, which flow below dry bars within the active channel, and floodplain fluxes, which include inter-meander fluxes and preferential flow paths along paleochannels [5]. Downwelling water then reemerges into the stream at upwelling areas after flowing within the streambed sediment for a residence time that depends on the spatial and temporal variations of the above

physical properties. In gravel bed rivers, near-bed pressure distribution is probably the main mechanism driving hyporheic exchange [7-10]. This distribution depends on the interaction between surface flow and streambed topography [1, 2] at different spatial scales [11]. Small-scale topography, such as dune-like bed forms, causes dynamic head variations which generate low pressure downstream from the dune crests, where flow detaches, and high pressure along dune stosses, where flow reattaches [12-14]. Conversely large-scale topography, such as pool-riffle sequences, influences water surface elevation and thus the piezometric head, which is the sum of the pressure and elevation heads, with relatively small effects on the dynamic head, at least at high and moderate flows [9]. Most hyporheic research has focused on hyporheic exchange induced by the micro or the macro scale topography separately, and only recently have models been proposed to superpose the effects of multiples scales [11, 15].

Hyporheic exchange models that include effects of both large and small scale topography are important, because they provide tools to study hyporheic exchange properties at the scale of the stream network. Because hyporheic exchange controls the amount of surface water mixed with the pore water and the residence time of mixing, the path lengths and fluxes of the hyporheic flows influence the water quality in the sediment interstices and the distribution of aerobic and anaerobic conditions within the streambed [4, 16, 17]. Consequently, mapping the fluxes and residence time distributions of the hyporheic zone is an important part of quantifying the impact of flow discharge on the benthic and streambed environment [18-21].

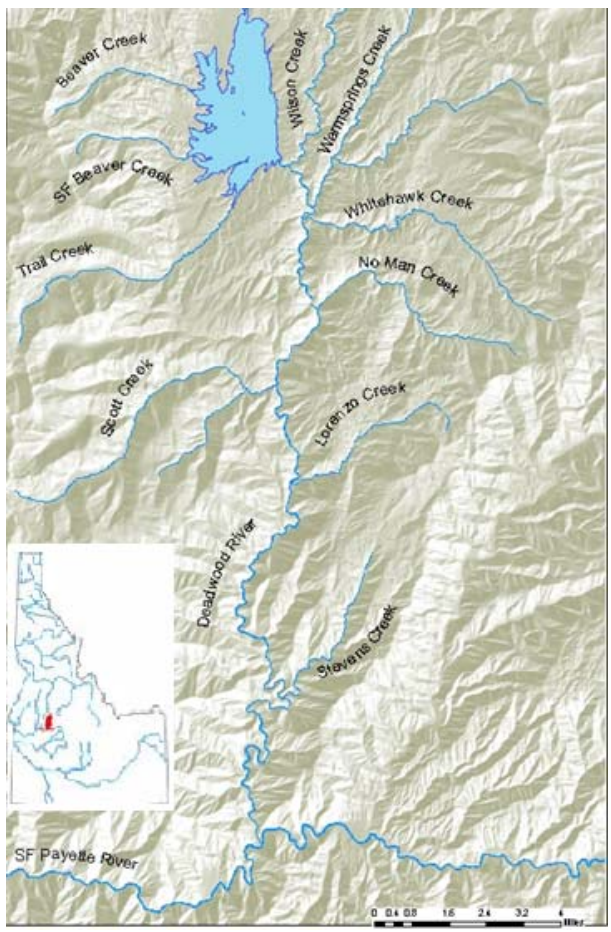

Figure 1. Lower section of the Deadwood River (Central Idaho, USA) between Deadwood Reservoir and the South Fork of the Payette River with the 7 major tributaries Wilson Creek, Warmsprings Creek, Whitehawk Creek, No Man Creek, Scott Creek, Lorenzo Creek and Stevens Creek. The scale bar is in miles. You could put the lat/long on the small inset figure, but probably not critical if you're out of time.

Whereas most hyporheic research focuses at the morphological unit (10^{-1}-10 times the channel width) and at the channel-reach scale (10-10^2 times the channel width) [21-25], here we investigate the spatial distribution of hyporheic exchange at the valley scale (10^3-10^4 times the channel width) along a 35km long river segment of the Deadwood River (Central Idaho, USA) (Figure 1). The objective of this study is to quantify the effect of flow discharge on hyporheic exchange at the valley scale. We develop a hyporheic hydraulic model by coupling the

dynamic and piezometric near-bed energy heads. The former is modeled as velocity head losses due to dune-like bed form, whose amplitude and wavelength is derived from wavelet analysis of the small-scale topography along the streambed centerline, the latter as the variation of the water surface elevations predicted by 1-dimensional hydraulic modeling.

2 STUDY SITE

The study site is the lower 37km-long section of the Deadwood river between Deadwood Reservoir and the confluence with the Payette river (Idaho, USA) (Figure 1). The channel has a mean width of 30m and coarse substrate dominated by cobbles and large gravel, d_{50} approximately 0.2 m. Fine sediment, fine gravel and sand, is limited to only a few patches within a few kilometers downstream of the confluence with one tributary. This portion of the Deadwood River flows in a narrow and deep canyon with the canyon walls largely defining the river sinuosity and restricting any inter-meander groundwater connectivity. The floodplain is also quite restricted with a few small exceptions. Consequently, the major component of the hyporheic flux is the fluvial hyporheic with the parafluvial and floodplain hyporheic exchanges negligible in this system.

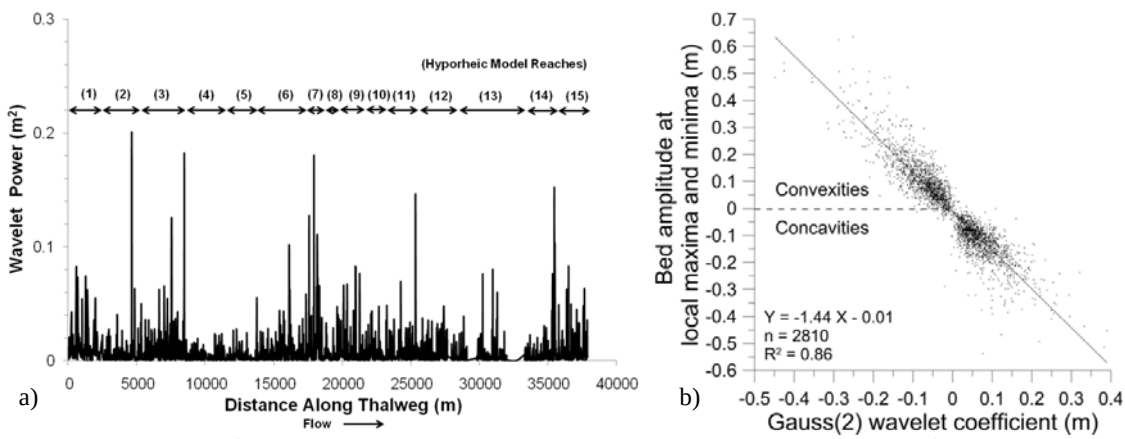

Figure 2. Wavelet analysis of the streambed topography along the river centerline. (a) shows the wavelet power for the 3m scale wavelet along the Deadwood river and (b) the relationship between bed amplitude and wavelet coefficient. This information was used to quantify the averaged small-topography amplitude over channel lengths corresponding to about 1 channel width.

Deadwood Reservoir regulates the stream discharge, which is augmented by 7 large and several small tributaries (Figure 1). Reservoir outflow dominates the stream discharge during the irrigation period (June-August), while tributary discharge dominates during April-June and tributary contributions equal the reservoir discharge in the rest of the year. The stream bathymetry was derived from data collected with the aquatic-terrestrial Experimental Advanced Airborne Research Lidar (EAARL) system in 2007 [26]. The lidar data density was approximately 0.6 points per square meter, from which a 3m grid digital elevation model (DEM) of the stream was derived. The DEM was used as the boundary condition for a 1-dimensional hydraulic model of surface flow and to extract information on the small-scale topography. We used a wavelet analysis of the topography along the stream centerline with a 3m-scale2nd derivative Gaussian reference wavelet to quantify the amplitude of the streambed small-scale topography for the hyporheic model (Figure 2) [26]. We used the wavelet power to divide the stream in reaches with homogenous small-scale amplitude. This analysis predicted 15 relatively homogeneous reaches (Figure 2). We used these reaches to investigate the effect of stream topography on hyporheic response at different discharges.

Table 1. Discharge scenarios modeled in the analysis

Scenario	Reservoir Releases [m3/s]	Date Range
1. Winter	0	5-1-2009 --> 24-2-2009
2. Winter	0.05	5-1-2009 --> 24-2-2009
3. Winter	1.42	5-1-2009 --> 24-2-2009
4. Spring: pre ramping	11.33	20-6-2009--> 5-7-2009
5. Spring: ramping	16.42	15-7-2009--> 20-7-2009
6. Summer: high flow	27.18	4-8-2009 --> 27-8-2009

3 METHOD

3.1 Surface flow modeling

Surface water hydraulics was modeled with a 1-dimensional hydraulic model (MIKE11®). Time series of measured outflows from the reservoir and discharges measured at the major tributaries were used as inflow boundary conditions and the downstream boundary is set as a discharge-stage rating curve. Cross-sections were extracted from the stream DEM every 30 m along the centerline to define the channel flow geometry. Calibration of flow resistance produced a value of Manning's n equal to 0.06 for the entire reach. Calibration was performed at a low flow condition when some, but limited, water surface elevations were available. The inaccessibility of the stream during high flows and for most of its course even at low flows, coupled with poor reception for obtaining precise GPS location and elevation measurements, reduces the possibility to gather data for calibration. The model was run for 6 scenarios, which are summarized in Table 1. These scenarios are based on the annual pattern of reservoir releases and bound the flow regime of the system. Discharge increases downstream as tributaries enter the main stem of the Deadwood River and their contributions vary during the year.

3.2 Hyporheic flow modeling

We assumed that in this confined mountain river the stream banks are impermeable and the alluvial depth, z_d, is 1 meter. Because of limited lateral exchange and mostly longitudinal variations of the streambed, we also assumed that transversal head variations are negligible. Consequently, hyporheic exchange chiefly varies longitudinally such that we can simplify the hyporheic flow as a 2-dimensional problem, along the vertical and longitudinal directions. We assumed a homogenous and isotropic hydraulic conductivity and steady-state conditions, such that the governing equation of the hyporheic flow is the Laplace equation:

$$\nabla^2 h_T = 0 \tag{1}$$

where h_T is the energy head. To solve this equation, we set the bottom boundary as impervious at a depth z_d and the upstream and downstream boundary as an energy drop equal to the streambed slope. The water-sediment boundary was set along the mean streambed elevation [1] and equal to the near-bed pressure distribution h_T. The following system of equations summaries our boundary conditions:

$$\begin{cases} h(0,z) = 0 \\ h_T(x,0) = h_s(x,0) + h_L(x,0) + h_{slope}(x) \\ \left.\frac{\partial h}{\partial z}\right|_{z=-z_d} = 0 \end{cases} \tag{2}$$

The total energy is the sum of: a) the energy head induced by small-scale topography, h_s, i.e. boulders and/or pebble clusters, which is modeled as dune-like head losses, b) large-scale topography, h_L, which is modeled as water surface elevation variations, and c) the streambed mean slope h_{slope}.

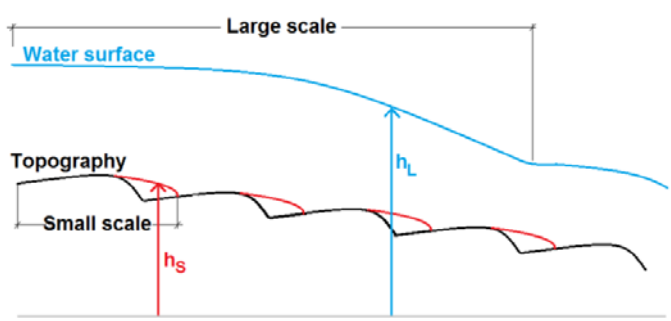

Figure 3. Effect of small, h_s, and large, h_L scale topography on near-bed pressure heads $h=h_s+h_L$

Head variation induced by small scale topography

The near-bed head variations due to small scale topography are modeled as dynamic head losses due to dune-like bed forms following the model of Stonedahl et al. [11]. They propose the following equation for the amplitude of head distributions, h_m

$$h_m = 0.28\frac{V^2}{2g\sqrt{2}\sigma_b}\begin{cases}\left(\frac{2\sqrt{2}\sigma_b}{0.34Y_0}\right)^{3/8} if\ \frac{2\sqrt{2}\sigma_b}{Y_0} \leq 0.34 \\ \left(\frac{2\sqrt{2}\sigma_b}{0.34Y_0}\right)^{3/2} if\ \frac{2\sqrt{2}\sigma_b}{Y_0} > 0.34\end{cases} \quad (3)$$

where V is the mean stream velocity, g is the gravitational acceleration, Y_0 is the mean flow depth, and σ_b is the mean amplitude of the small-scale topography at the reach scale. The 1-dimensional hydraulic model of the surface flow provides the local values of V and Y_0 for the 6 discharges. The head distributions induced by the small-scale topography at the streambed interface are then represented in terms of a Fourier analysis of the bed amplitude oscillations modulated by h_m:

$$h_S(x,0) = 2h_m \sum_{i=1}^{N} a_{S,i} sin\left(\frac{2\pi i}{L}x - \varphi_{s,i}\right) \quad (4)$$

where $a_{S,i}$ and $\varphi_{S,i}$ are the amplitudes and the phases of the topography data of Fourier harmonics, respectively. N is the number of harmonics considered in the expansion along the longitudinal direction, L is the reach length and x is the longitudinal direction. The number of harmonics considered in the expansion along the longitudinal direction is set to be one less than half of the number of data points to comply with the Nyquist frequency cutoff.

Head variations induced by large scale topography

The near-bed head distribution induced by large-scale topography was modeled in terms of the Fourier series of the water surface elevation:

$$h_L(x,0) = 2\sum_{i=1}^{M} \mathrm{a_{L,i}} \sin\left(\frac{2\pi i}{L}x - \varphi_{L,i}\right) \quad (5)$$

where $a_{L,i}$ and $\varphi_{L,i}$ are the amplitudes and the phases of the water surface elevation of Fourier harmonicas, respectively and M is the number of harmonics considered in the expansion along the longitudinal direction. Because the Laplace equation is linear, we can superpose the contribution of each factor independently:

$$h_T(x,0) = h_S(x,0) + h_L(x,0) + h_{slope}(x) \quad (6)$$

where h_{slope} is the head distribution due to the mean streambed slope (s_0).
The solution for the equation (1) with the boundary and initial conditions expressed by equations (2), (3) and (6) is:

$$h(x,z) = 2h_m \sum_{i=1}^{N} a_{S,i} \sin\left(\frac{2\pi i}{L_S}x - \varphi_{S,i}\right)\left[\tanh\left(\frac{2\pi i}{L}z_d\right)\sinh\left(\frac{2\pi i}{L}z\right) + \cosh\left(\frac{2\pi i}{L}z\right)\right] + 2\sum_{i=1}^{M} a_{L,i} \sin\left(\frac{2\pi i}{L}x - \varphi_{L,i}\right)\left[\tanh\left(\frac{2\pi i}{L}z_d\right)\sinh\left(\frac{2\pi i}{L}z\right) + \cosh\left(\frac{2\pi i}{L}z\right)\right] + xs_0 \quad (7)$$

Once the pressure distribution is known within the hyporheic zone, we compute the velocity field with Darcy's equation (equation (8)), which relates velocity with the gradient of the pressure head:

$$u(u,w) = -\frac{K}{\phi}\frac{\partial h}{\partial x}, -\frac{K}{\phi}\frac{\partial h}{\partial z} \quad (8)$$

where ϕ is the sediment porosity, which we set equal to 0.34. Because of the coarse material and low percent of fine grains, we set the hydraulic conductivity, K=0.01 m/s. The hyporheic flow velocity components are then:

$$u(x,z) = -2h_m \frac{K}{\phi}\sum_{i=1}^{N}\frac{2\pi i}{L_S} a_{S,i}\cos\left(\frac{2\pi i}{L}x-\varphi_{S,i}\right)\left[\tanh\left(\frac{2\pi i}{L}z_d\right)\sinh\left(\frac{2\pi i}{L}z\right)+\cosh\left(\frac{2\pi i}{L}z\right)\right] - 2\frac{K}{\phi}\sum_{i=1}^{M}\frac{2\pi i}{L} a_{L,i}\cos\left(\frac{2\pi i}{L}x-\varphi_{L,i}\right)\left[\tanh\left(\frac{2\pi i}{L}z_d\right)\sinh\left(\frac{2\pi i}{L}z\right)+\cosh\left(\frac{2\pi i}{L}z\right)\right] - \frac{K}{\phi}s_0 \quad (9)$$

$$v(x,z) = -2h_m \frac{K}{\phi}\sum_{i=1}^{N}\frac{2\pi i}{L_S} a_{S,i}\sin\left(\frac{2\pi i}{L}x-\varphi_{S,i}\right)\left[\tanh\left(\frac{2\pi i}{L}z_d\right)\cosh\left(\frac{2\pi i}{L}z\right)+\sinh\left(\frac{2\pi i}{L}z\right)\right] - 2\frac{K}{\phi}\sum_{i=1}^{M}\frac{2\pi i}{L} a_{L,i}\cos\left(\frac{2\pi i}{L}-\varphi_{L,i}\right)\left[\tanh\left(\frac{2\pi i}{L}z_d\right)\cosh\left(\frac{2\pi i}{L}z\right)+\sinh\left(\frac{2\pi i}{L}z\right)\right] \quad (10)$$

Once the flow field is known, the hyporheic residence time and the mean upwelling fluxes are predicted with the particle tracking technique [27]. The mean upwelling flux for each stream reach is calculated with the following integral, which is a weighted mean of the fluxes within a reach:

$$\overline{q}_{uw} = \frac{1}{A_{uw}}\int_A u_{uw}\,\phi dA_{uw} \quad (11)$$

4 RESULTS

Figure 4 shows the distribution of the mean upwelling flux, q_{uw}, (Figure 4a) and mean residence time distribution τ_{ave} (Figure 4b) for the 15 reaches of the Deadwood River which are arranged by progressive distance from the reservoir. The distribution of the mean upwelling fluxes has the same trend and magnitude for all scenarios regardless of stream discharge. Mean fluxes vary between 5 to $33\cdot10^{-5}$ m/s depending on local h_m. Reaches with large fluxes coincide with those sections with large dynamic head amplitude, h_m. Conversely, the trend of the mean hyporheic residence time shows long residence times in reaches with low h_m and short residence time in reaches with large h_m. The effect of discharge on τ_{ave} is only visible in a few reaches (3, 4, 5 and 14) where residence times decrease with increasing discharge. The mean hyporheic residence time decreases with increasing discharge and in reach 5 at 960 cfs the residence time is approximately half that at 50 cfs.

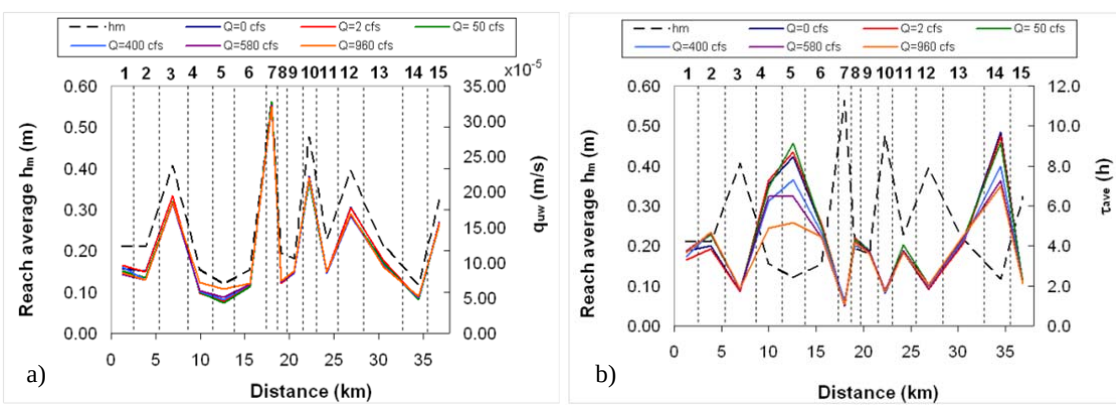

Figure 4. Spatial trend of (a) the upwelling fluxes and (b) hyporheic residence time distribution as a function of discharge for the 15 reaches along the Deadwood River

5 DISCUSSION

Inspection of equation (3) shows that the head amplitude should increase with velocity and decrease with water depth. Because the Deadwood River is a wide stream, we expect that velocity should increase faster than the

water depth such that the net discharge effect is that hyporheic fluxes should increase with discharge for the small-scale topography. Conversely, water surface elevation variations should decrease with discharge, because local topography as it is drowned by the flow has less influence on the water surface elevation. We also expected that the head variations generated by the large-scale topography would dominate those induced by the small-scale topography. Consequently, our expectation was that fluxes would have decreased and mean hyporheic residence time would have increased with discharge. Our results show a different process. Discharge increases have negligible effects on the hyporheic fluxes and it may be that changes in flow characteristics such as depth, water surface elevation and mean velocity, associated with increases in discharge, cancel out each other effects in this system. Unexpectedly, we see a decrease of residence time distribution with discharge. This could be explained by the interplay between reductions in head amplitude and path length. As discharge increases, head variations decrease all but the head associated with the streambed slope, h_{slope}, which remains constant. Consequently, hyporheic flow paths remain closer to the streambed surface. This process reduces their lengths and compensate for the reduction of head variations. The net result is that the overall energy slope remains constant.

6 CONCLUSIONS

Advances in remote survey techniques, in numerical modeling, and in conceptual modeling of the surface-subsurface flow interaction allowed us to investigate the hyporheic exchange along a 35km-long river section. Our analysis accounted for longitudinal variations of surface water hydraulic properties, streambed elevation, and hyporheic fluxes induced by small-scale and large-scale topographic elements. Our results show that discharge has a negligible effect on hyporheic fluxes in this domain, but may influence the mean hyporheic residence time. The latter is an important index for aerobic and anaerobic conditions within the streambed sediment. Our analysis shows that large discharges decrease the mean hyporheic residence time only in 4 out of 15 morphologically homogenous reaches. In the other reaches, discharge has a negligible effect on hyporheic fluxes. Small-scale topography seems to explain most of the variability in hyporheic fluxes. Reaches with large amplitude, h_m, of the head distribution induced by the small-scale topography are characterized by large fluxes and short residence time while reaches with small h_m have small fluxes and long hyporheic residence times.

6.1 Acknowledgments, appendices, and references

This research was partially funded by the US Forest Service Grant 08-JV-11221659-036.

6.2 References

[1] Elliott, A. and N.H. Brooks, "Transfer of nonsorbing solutes to a streambed with bed forms: theory", *Water Resources Research*, Vol. 33, No. 1, (1997), pp 123-136.

[2] Elliott, A. and N.H. Brooks, "Transfer of nonsorbing solutes to a streambed with bed forms: laboratory experiments", *Water Resources Research*, Vol. 33, No. 1, (1997), pp 137-151.

[3] Tonina, D. and J.M. Buffington, "Hyporheic exchange in mountain rivers I: Mechanics and environmental effects ", *Geography Compass*, Vol. 3, No. 3, (2009), pp 1063 - 1086.

[4] Tonina, D., A. Marzadri, and A. Bellin. "Effect of hyporheic flows induced by alternate bars on benthic oxygen uptake". *34th IAHR World Congress 2011*, Brisbane, Australia, (2011), pp 3129-3136.

[5] Edwards, R.T., "The hyporheic zone", in *River ecology and management: Lessons from the Pacific coastal ecoregion*, R.J. Naiman and R.E. Bilby, Editors, Springer-Verlag, (1998), p. 399-429.

[6] Boano, F., D. Poggi, R. Revelli, and L. Ridolfi, "Gravity-driven water exchange between streams and hyporheic zones", *Geophysical Research Letters*, Vol. 36, (2009), pp L20402.

[7] Gooseff, M.N., J.K. Anderson, S.M. Wondzell, J. LaNier, and R. Haggerty, "A modelling study of hyporheic exchange pattern and the sequence, size, and spacing of stream bedforms in mountain stream networks, Oregon, USA", *Hydrological Processes*, Vol. 20, No. 11, (2006), pp 2443-2457.

[8] Gooseff, M.N., R.O.J. Hall, and J.L. Tank, "Relating transient storage to channel complexity in streams of varying land use in Jackson Hole, Wyoming", *Water Resources Research*, Vol. 43, No. W01417, (2007).

[9] Tonina, D. and J.M. Buffington, "Hyporheic exchange in gravel-bed rivers with pool-riffle morphology: laboratory experiments and three-dimensional modeling", *Water Resources Research*, Vol. 43, No. W01421, (2007).

[10] Tonina, D. and J.M. Buffington, "Effects of stream discharge, alluvial depth and bar amplitude on hyporheic flow in pool-riffle channels", *Water Resources Research*, Vol. 47, (2011), pp W08508.

[11] Stonedahl, S.H., J.W. Harvey, A. Wörman, M. Salehin, and A.I. Packman, "A multi-scale model for integrating hyporheic exchange from ripples to meanders", *Water Resources Research*, Vol. 46, (2010), pp W12539.

[12] Savant, A.S., D.D. Reible, and L.J. Thibodeaux, "Convective Transport Within Stable River Sediments", *Water Resources Research*, Vol. 23, No. 9, (1987), pp 1763-1768.

[13] Vittal, N., K.G. Ranga Raju, and R.J. Garde, "Resistance of two-dimensional triangular roughness", *Journal Hydraulic Research*, Vol. 15, No. 1, (1977), pp 19-36.

[14] Thibodeaux, L.J. and J.D. Boyle, "Bedform-generated convective transport in bottom sediment", *Nature*, Vol. 325, No. 22, (1987), pp 341-343.

[15] Wörman, A., A.I. Packman, L. Marklund, and J.W. Harvey, "Exact three-dimensional spectral solution to surface-groundwater interaction with arbitrary surface topography", *Geophysical Research Letters*, Vol. 33, No. L07402, (2006).

[16] Marzadri, A., D. Tonina, and A. Bellin, "A semianalytical three-dimensional process-based model for hyporheic nitrogen dynamics in gravel bed rivers", *Water Resources Research*, Vol. 46, (2011), pp W11518.

[17] Zarnetske, J.P., R. Haggerty, S.M. Wondzell, and M.A. Baker, "Dynamics of nitrate production and removal as a function of residence time in the hyporheic zone", *Journal of Geophysical Research*, Vol. 116, (2011), pp G01025.

[18] Kasahara, T., T. Datry, M. Mutz, and A.J. Boulton, "Treating causes not symptoms: restoration of surface-groundwater interactions in rivers", *Marine and Freshwater Research*, Vol. 60, (2009), pp 976-981.

[19] Kasahara, T. and A.R. Hill, "Effects of riffle–step restoration on hyporheic zone chemistry in N-rich lowland streams", *Canadian Journal of Fisheries and Aquatic Sciences*, Vol. 63, (2006), pp 120-133.

[20] Kasahara, T. and A.R. Hill, "Hyporheic exchange flows induced by constructed riffles and steps in lowland streams in southern Ontario, Canada", *Hydrological Processes*, Vol. 20, (2006), pp 4287-4305.

[21] Kasahara, T. and A.R. Hill, "Lateral hyporheic zone chemistry in an artificially constructed gravel bar and a re-meandered stream channel, Southern Ontario, Canada", *Journal of the American Water Resources Association*, Vol. 43, No. 5, (2007).

[22] Cardenas, M.B., J.F. Wilson, and V.A. Zlotnik, "Impact of heterogeneity, bed forms, and stream curvature on subchannel hyporheic exchange", *Water Resources Research*, Vol. 40, No. W08307, (2004).

[23] Wörman, A., A.I. Packman, H. Johansson, and K. Jonsson, "Effect of flow-induced exchange in hyporheic zones on longitudinal transport of solutes in streams and rivers", *Water Resources Research*, Vol. 38, No. 1, (2002), pp 15.

[24] Marion, A., M. Zaramella, and A. Bottacin-Busolin, "Solute transport in rivers with multiple storage zones: The STIR model", *Water Resources Research*, Vol. 44, (2008), pp W10406.

[25] Marion, A., M. Bellinello, I. Guymer, and A.I. Packman, "Effect of bed form geometry on the penetration of nonreactive solutes into a streambed", *Water Resources Research*, Vol. 38, No. 10, (2002), pp 1209.

[26] McKean, J.A., D. Nagel, D. Tonina, P. Bailey, C.W. Wright, C. Bohn, and A. Nayegandhi, "Remote sensing of channels and riparian zones with a narrow-beam aquatic-terrestrial LIDAR", *Remote Sensing*, Vol. 1, (2009), pp 1065-1096.

[27] Tonina, D. and A. Bellin, "Effects of pore-scale dispersion, degree of heterogeneity, sampling size, and source volume on the concentration moments of conservative solutes in heterogeneous formations", *Advances in Water Resources*, (2007).